Orbital: The Electronic Journal of Chemistry
journal homepage: www.orbital.ufms.br
ISSN 1984-6428

| Vol 9 | | No. 4 | | July-September 2017 |

Full Paper.

Structural and Magnetic Characterization of Nanostructured Iron Acetate

Antônio Oliveira de Souza[a*], Valdecir Biondo[b], Flávio Francisco Ivashita[b], Glécilla Colombelli de Souza Nunes[b], and Andrea Paesano Jr.[b]

[a]*Universidade Federal do Oeste da Bahia, Centro Multidisciplinar do Campus de Bom Jesus da Lapa, Avenida Manoel Novaes nº 1064, CEP 47600-000, Bom Jesus da Lapa - BA, Brasil.*
[b]*Departmento de Física, Universidade Estadual de Maringá, Avenida Colombo nº 5790, CEP 87020-900, Maringá - PR, Brasil.*

Article history: Received: 29 May 2017; revised: 14 August 2017; accepted: 14 August 2017. Available online: 26 September 2017. DOI: http://dx.doi.org/10.17807/orbital.v9i4.1006

Abstract: Iron(II) acetate anhydrous, (i) as received (FeAc) and (ii) processed by freeze-drying (FeAc-FD), were characterized structural, magnetic and morphologically by thermal analysis, scanning electron microscopy, thermogravimetry, differential scanning calorimetry and X-ray diffraction. As a result of these analyzes, it was found that the FeAc- FD type leaves showed a morphology with a thickness in the nanometer scale. The activation energy (E_a) for the exothermic events related to the decomposition of the above acetate was estimated in the range of 275-328 °C. Values for E_a equal to 100,225 and 127,824 kJ / mol were obtained for the FeAc and FeAc-FD, respectively. Mössbauer spectra showed as isomer shift (IS) characteristic of a Fe^{+3} to the FeAc-FD, and Fe^{+3} and Fe^{+2} to the FeAc. The results indicate that freeze-drying of FeAc could be used as a precursor to further processing method of decreasing the synthesis temperature.

Keywords: activation energy; freeze-drying; nanostructured iron(II) acetate; termogravimetry and differential scanning calorimetry; spectroscopy Mössbauer

1. INTRODUCTION

Among other cations of transition metals, iron cations are widely used for doping of several semiconductors, due to its high magnetic moment and possibility of characterization by Mössbauer spectroscopy. By replacing a small fraction of the non-magnetic cations (i.e., Zn^{+2} of the ZnO) by magnetic cations (i.e., Fe^{+3} / Fe^{+2} / Mn^{+2}) it is possible to dilute magnetic moments in the host semiconductor lattice. There is great interest in these materials because they represent a new class of semiconductors called Dilute Magnetic Semiconductors (DMS) [1], which can plausibly exhibit ferromagnetism at room temperature [2]. These compounds would be of high technological applicability in spintronics [3]. In this sense, the aim of accelerating Mössbauer spectroscopy measurements, obtaining well-resolved spectra for DMS's, De Souza et al. synthesized the iron acetate enriched in the ^{57}Fe isotope [4].

Iron acetates are highly soluble in water and may easily decompose in nanostructured iron oxides [5] under appropriate heat treatments up releasing H_2O, acetic acid, acetone and CO_2. The thermal decomposition of iron or other inner transition metal acetates under different heat treatment conditions may lead to formation of several ultrafine oxides [6-8] with high technological applicability [9]. Some results for iron(III) [10] or iron(II) [11] acetates have shown that interesting magnetic and structural properties can be obtained from such relatively simple compounds. Jewur and Kuriacose [12] performed a systematic study of the thermal decomposition of ferric acetate that shows it decomposes to the hematite phase with activation energy of 94.98 kJ/mol.

In the present study, it was used the freeze-drying method in the processing of the precursor (FeAc). This technique is frequently used to dehydrate aqueous mixes resulting in a final product which maintaining the basic structure of the initial salt with fine or ultrafine solid particles that shows high homogeneity and chemical reactivity [13-15]. Any modification in mass of the sample is usually related to the water loss.

*Corresponding author. E-mail: antonio.oliveira@ufob.edu.br

Taking advantage of the above-mentioned characteristics of acetates, a mixture of two (or more) acetates can also be processed (i.e., freeze-dry and thermally treated) to form a nanometric ceramics, stoichiometric composition or, optionally, cations of a metal in solid solution in the host matrix of another metal [4]. For example, when we make a mixture of the iron acetate with the zinc acetate freeze-dried and heat treated, result in ZnFeO solid solution magnetically doped.

The main purpose of this work was to characterize the morphology, the magnetic and structural properties of nanostructured iron acetate produced by freeze-drying. For to characterize the acetates (i.e., FeAc and FeAc-FD), we used Mössbauer Spectroscopy, X-Ray Diffraction (XRD), Thermogravimetric Analysis/Differential Scanning Calorimetry (TGA-DSC) and Scanning Electron Microscopy (SEM).

2. MATERIAL AND METHODS

2.1 Sample preparation and Freeze-drying

Initially, the commercial iron(II) acetate, $Fe(CH_3COO)_2$ (FeAc), was homogeneously diluted in 20 ml of distilled-deionized water at room temperature (RT). Subsequently, the aqueous mixture was placed inside a glass flask in rotation and slowly frozen by immersion in liquid nitrogen. Finally, the flask was connected to the freeze-drying which consisted of a vacuum pump (Liotop, IP21) and a water trap (Liotop, L101). During the stage of freeze-dryer, the frozen sample was sublimed under low pressure (~ 250 μmHg) and temperature (-58 °C). The process for complete drying of the samples took approximately 14 hours resulting in a dry powder (FeAc-FD). After, all powders were subjected to heat treatment dynamic in an air synthetic atmosphere in a range of temperature of 22 °C until 600 ºC.

2.2 Characterization techniques

X-ray diffraction

The crystalline structure of the as-received and freeze-dried acetates was determined by XRD, in a Shimadzu diffractometer (XRD-6000) at room temperature and working in the conventional geometry (i. e., Bragg-Brentano, θ - 2θ). It was utilized Kα of the copper tube (λ = 1.5406 Å) with tension of 40 kV and filament current of 30 mA. The diffractograms were taken in a range of $5° \leq 2\theta \leq 80°$ with 0.02° and 5 s per step.

Scanning electron microscopy

To analyze the morphological aspect of the samples it has been used the Scanning Electron Microscopy technique (SEM) in a Shimadzu microscopy (SS 550 Superscan).

Thermal analysis

The thermal decomposition of the FeAc and FeAc-FD acetates (samples with mass around 9 mg contained in an alumina crucible) was studied by TGA/DSC techniques in a Netzsch thermal analyzer (model STA 409 PG/4/G Luxx) with synthetic air atmosphere (N_2 = 80% in flux of 40 mL/min.; O_2 = 20% in flux of 10 mL/min.). It was used the measurement of the empty crucible as reference to the baseline (to both TGA and DSC). The temperature was raised from RT (room temperature) up to 600 °C with five different rates of heating: β = 4, 8, 12, 16 and 20 °C/min.

Spectroscopy Mössbauer

The Mössbauer ^{57}Fe spectra were taken at RT by using a conventional spectrometer with source of $^{57}Co(Rh)$ moved in horizontal with a constant acceleration. The absorber was prepared to contain about 20 mg/cm² of iron acetate. It was utilized a spectrum of zero-valent α-Fe taken at room temperature for the calibration of the equipment.

3. RESULTS AND DISCUSSION

Figure 1 shows the X-ray diffractograms for the acetates (FeAc and FeAc-FD). The XRD of FeAc, Figure 1.a, shows well-defined crystalline peaks at low angles. On the other hand, the FeAc-FD presents a very different pattern of diffraction (Figure 1.b) from the one showed in the Figure 1.a. This indicates some reduction on crystallinity and a possible structural change of the freeze-dried acetate when compared to the acetate as received.

Figure 2 shows the microstructure of as-received (2.a and 2.b) and freeze-dried (2.c and 2.d) iron acetates in different magnifications. It is possible to see, by visual inspection, that the as-received iron acetate presented a preferably cylindrical morphology

with diameters between 1 and 15 μm. However, for the freeze-dried iron acetate, it is possible to see a preferential nanosheets morphology with average thickness in nanoscale (i.e., < 100 nm). Around these results, we can conclude that the freeze-drying process modify both average size and shape of the precursor, leading the samples to the nanoscale that causes alterations in their physical and chemical properties making them more reactive [9]. Once the freeze-dried material has very little available water between acetate bonds, such alterations can be justified by the fact that the superficial area of the formed solid depends on the availability of water during the dehydration process [16].

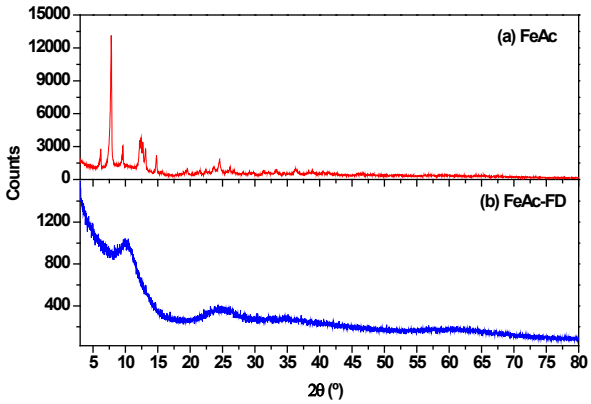

Figure 1. X-Ray diffractograms for the acetate samples: (a) FeAc; (b) FeAc-FD.

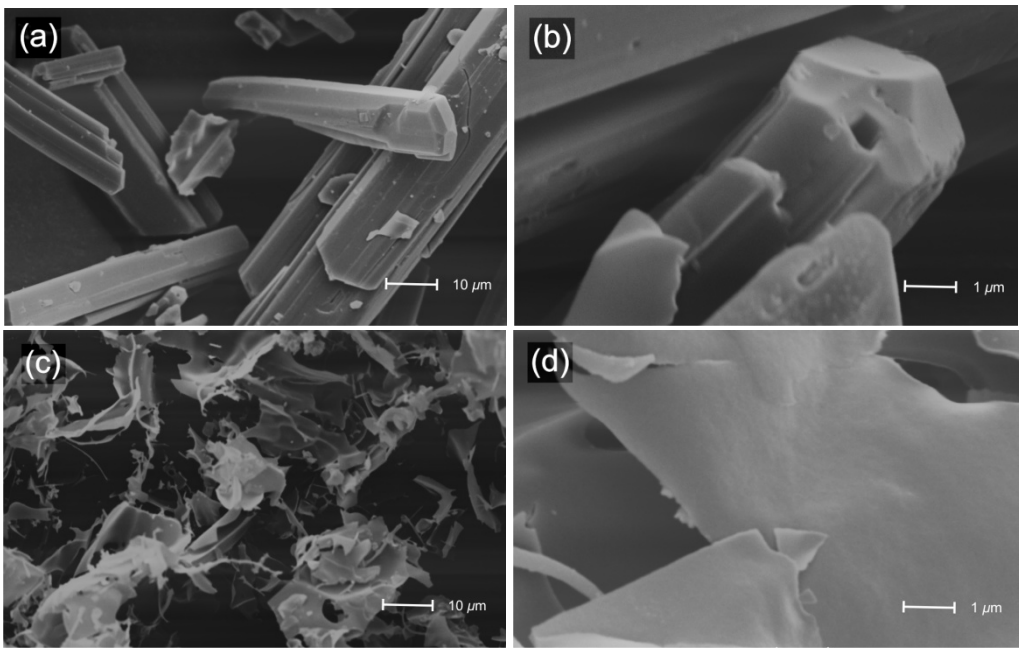

Figure 2. Acetate microstructures: (a) and (b) FeAc; (c) and (d) FeAc-FD.

The Figure 3 shows the results of TGA/DSC analysis with heating rates β = 4, 8, 12, 16 and 20 °C/min for the acetates FeAc and FeAc-FD. It can be deduced that the endothermic events (in DSC) which occurred between 22 °C and 260 °C are associate to the decomposition of FeAc. The exothermic event with well-defined sharp peaks that occurred between 260 °C and 600 °C corresponds to the sample thermal decomposition, leading to formation of iron oxides. A verification of the TGA/DSC curves in Figure 3 reveals that the peaks move to higher temperatures when increased the heating rate and it complies with the law of general rate [17]. This shift to the right as the heating rate increases is also observed in the TGA curves. This may be attributed to the higher surface energy [8] of the large surface area in FeAc-FD.

Accordingly, to the heating rates of 4, 8, 12, 16 and 20 °C/min, the exothermic event for FeAc has shown maximum peaks around T_β = 286 °C, 304 °C, 312 °C, 320 °C, and 328 °C, respectively. For the exothermic event of FeAc-FD, characterized by the same heating rates, the maximum peaks occurred around T_β = 275 °C, 292 °C, 299 °C, 302 °C e 306 ºC, respectively. One can see that in the exothermic events, the peak temperatures for FeAc-FD were lower than FeAc when we compare both of them regardless of the heating rate.

Figure 3.a shows that the mass loss observed at 400 °C (with rate β = 12 °C/min) in TGA curve of FeAc was 61.6%. Considering the decomposition of a stoichiometric anhydrous iron(II) acetate, $Fe(CH_3COO)_2$, into hematite the theoretical loss

would be 54%. As we can see, there is a pronounced divergence between the experimental and theoretical results. Face of this deadlock the calculations were made using the experimental results and it was found that FeAc shouldn't have the structural formula as anhydrous, $Fe(CH_3COO)_2$, but a mix of acetates that contains Fe^{+2} and Fe^{+3} like $Fe(CH_3COO)_2{\cdot}Fe(CH_3COO)_3$. The theoretical mass loss for the mix of acetates is 61% that is very close to the experimental value obtained.

The TGA data from Figure 3.b measured at 400 °C and β = 12 °C/min shows that the thermal decomposition (200 °C to 600°C) occurred with a mass loss of 44,3% for the FeAc-FD. This value is considerably lower than the seen in FeAc sample, which can be attributed to the lower amount of absorbed water in the freeze-dried sample, compared to the as-received sample.

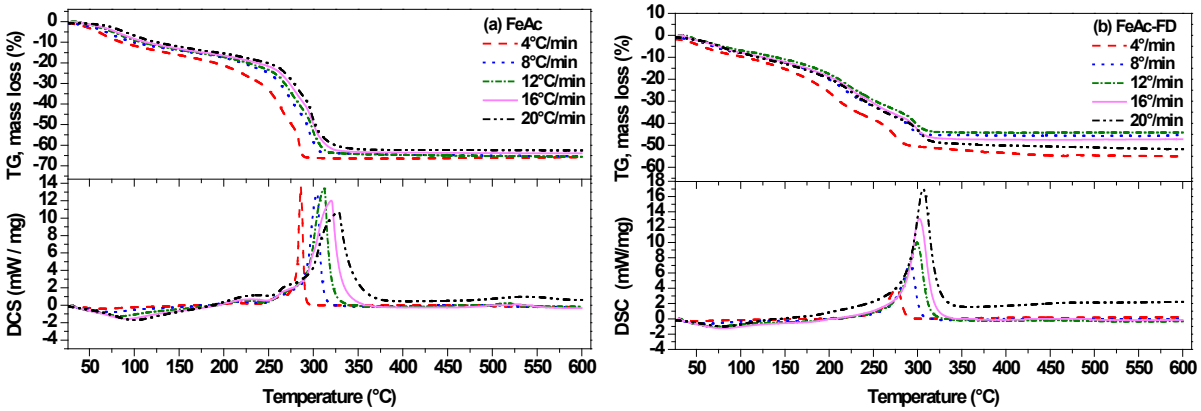

Figure 3. TGA/DSC curves obtained in different heating rates for acetates: (a) FeAc and (b) FeAc-FD.

As we can see in DSC graphs, the freeze-dried acetates decompose at lower temperatures, which may be related to the fine powder morphologies. In the FeAc graph (Figure 3.a) is seen a decrease of the exothermic peaks when the dynamic temperature increases and it may be associated with the larger particles of the material, while in the FeAc-FD (Figure 3.b) we can see an increase of the peaks when it increases the dynamic temperature, so it may be related to the smaller particles. These results can represent higher formation of hematite when it decreases the particles size [18].

Figure 4 shows the straight that allows us to calculate the activation energy (E_a) of the acetates. The calculated activation energy for the shown exothermic events, according to the standard ASTM E698-11[17], were obtained using the angular coefficients values with support of Arrhenius equation [19]. The obtained activation energy of FeAc was E_a = 100,225 kJ/mol. This value is close to the one obtained by Jewur and Kuriacose[7] for the ferric acetate (E_a = 94,98 kJ/mol). The activation energy for FeAc-FD was E_a = 127,824 kJ/mol.

The fact that the activation energy for the FeAc-FD is greater than for the FeAc could mean a greater sensitivity of the rate constant relative to temperature changes [19]. This observation is according to the seen results in DSC exothermic peaks, since for the FeAc-FD, the products were obtained at lower temperatures and it indicates that the freeze-dried material can be more reactive.

The activation energy values we got for FeAc and FeAc-FD are smaller than those ones found in scientific literature for some transition metal acetates [8]. Although the activation energy has been calculated only with the peaks of the exothermic event, the endothermic event occurred before can influence the total energy of the system, and this causes a lower activation energy for the AcFe due to the energy that was absorbed in the endothermic event.

The Mössbauer spectrum of the FeAc-FD acetate, obtained in 300 K, is presented in Figure 5. The spectrum of FeAc-FD was adjusted with a typical doublet of Fe^{+3}, i.e., δ =0,37 (mm/s), ΔE_q= 0,75 (mm/s) and Γ= 0,47 (mm/s). It was not possible to adjust the Mössbauer spectrum of the FeAc which can be attributed to the fact that the Mössbauer output file is corrupted. This would be a confirmation of the inhomogeneity of $Fe(CH_3COO)_2$, showing that there is in fact a mixture of acetates, containing iron in the ferrous and ferric states, as already discussed in the analysis DSC/TG.

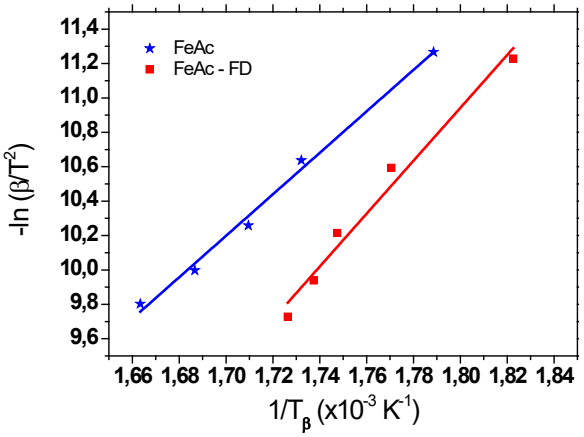

Figure 4. Graph for the Arrhenius' equation $K = Ae^{-\frac{E_a}{RT_\beta}}$, where $K = \beta$ is the rate constant, $A = T_\beta^2$ is the frequency factor, E_a is the activation energy, R is the ideal gases constant and T_β is the exothermic peaks temperature in Kelvin scale. The straights are numerical adjustment of the experimental points obtained by linear regression.

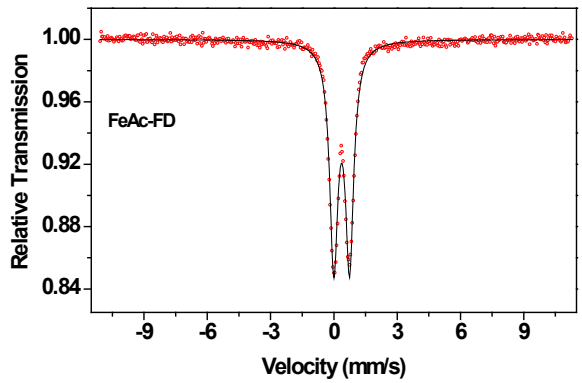

Figure 5. Mössbauer spectra of the FeAc-FD.

4. CONCLUSION

The results for the present investigation reveal that the Freeze-drying process changes the morphology of micrometric cylindrical for nanometric sheets of high aspect ratio. This process is also effective in total structural dehydration of iron(II) acetate. The initial acetate, after processing by freeze-drying, changed its crystal structure and oxidation state, from the initial ferrous to the ferric state. It was observed that the freeze-dried material produces solid products at lower temperatures, indicating greater reactivity, which may be explained by the high surface area powders. Calculations using Arrhenius equation provide us lower activation energy for AcFe due to the energy was absorbed in the endothermic event.

5. ACKNOWLEDMENTS

The authors thank CAPES for their financial support and also thank the Complex of Research Support Centers of the State University of Maringá for conducting some experiments.

6. REFERENCES AND NOTES

[1] Ohno, H. *Science* **1998**, *281*, 951. [CrossRef]

[2] Dietl, T.; Ohno, H.; Matsukura, F. *Phys. Rev. B.* **2001**, *63*, 195205. [CrossRef]

[3] Zutic, I.; Fabian, J.; Das Sarma, S. *Rev. Mod. Phys*. **2004**, *76*, 323. [CrossRef]

[4] de Souza A. O., Biondo, V.; Sarvezuk, P. W. C.; Bellini, J. V.; Anizelli, P. R.; Zaia, D. A. M.; Paesano Jr., A. *Quim. Nova* **2014**, *37*, 1132. [CrossRef]

[5] Silva, M. F.; Pineda, E. A. G..; Bergamasco, R. *Quim. Nova* **2015**, *38*, 393. [CrossRef]

[6] Seham, A. A. M.; Gamal, A. M. H.; Mohamed, I. Z. *React. Solids* **1990**, *8*, 197.

[7] Seham, A. A. M.; Gamal, A. M. H.; Mohamed, I. Z. *Thermochim. Acta* **1989**, *150*, 153. [CrossRef]

[8] Brown, M. E.; Dollimore, D.; Galwey, A. K.; Comprehensive Chemical Kinetics. Vol. 22, Amsterdam: Elsevier; 1980.

[9] Langbein, H.; Michalk, C.; Knese, K.; Eichhorn, P. *J. Eur. Cer. Soc*. **1991**, *8*, 171. [CrossRef]

[10] Yan-Zhen, Z.; Wei, X.; Ming-Liang, T.; Xiao-Ming, C.; Fernande, G.; Gary, J. L. *Inor. Chem.* **2008**, *46*, 6076. [CrossRef]

[11] Martin, V.; Peter, A.; Rodolphe, C.; Christopher, E. A.; Annie, K. P. *Eur. J. Inorg. Chem*. **2005**, *4*, 692. [CrossRef]

[12] Jewur, S. S.; Kuriacose, J. C.; Thermochim. Acta. 1977, 19, 195. [CrossRef]

[13] Bellini, J. V.; Medeiros, S. N.; Ponzoni, A. L. L.; Longen, F. R.; Melo, M. A. C.; Paesano Jr, A. Mater. Chem. Phys. 2007, 105, 92. [CrossRef]

[14] Louis, R.; Joan, C. M.; Freeze Drying/Lyophilization of pharmaceutical and Biological products. Third ed. London: Informa Healthcare, 2010.

[15] George-Wilhelm, O.; Peter, H. Freeze-Drying. Second ed. Weinheim: Wiley-VCH, 2004.

[16] Ball, M. C.; Norwood, L. S.; Reactivity of Solids. Proc. Seven ed. London: Chapman and Hall, 1972.

[17] STD - ASTM E698-ENGL. "Standard test method for Arrhenius kinetic constants for thermally unstable materials." ASTM International Standar, 1999.

[18] Robert, F. S.; Thermal analysis of materials. New York: Marcel Dekker, 1994.

[19] Atkins, P.; Jones, L.; Chemical Principles - The Quest for Insight. fourth ed. New York: W. H. Freeman, 2007.